DOI 10.1007/s11182-022-02658-6
Russian Physics Journal, Vol. 65, No. 3, July, 2022 (Russian Original No. 3, March, 2022)

PHYSICS OF SEMICONDUCTORS AND DIELECTRICS

OXIDATION OF CARBON MONOXIDE ON THE SURFACE OF A METAL OXIDE STRUCTURE

T. T. Magkoev,[2] I. V. Silaev,[2] O. G. Ashkhotov,[1,2] V. B. Zaalishvili,[3] and Z. T. Sozaev[2] UDC 544.723.5

The oxidation of carbon monoxide on the surface of the $Au/Al_2O_3/Mo(110)$ *structure was studied using modern methods of surface diagnostics. It is shown that at a high degree of identity of the structural, electronic, and adsorption properties of the* $Au/Al_2O_3/Mo(110)$ *system with various aluminum oxide film thicknesses (2, 4, 6, and 8 monolayers), the oxidation efficiency of* CO *molecules desorbed into the gas phase decreases exponentially with increasing oxide film thickness. Taking into account the well-known fact that the efficiency of* CO *oxidation depends on the amount of the excess charge acquired by the gold nanoparticle, it is concluded that charge tunneling through the oxide layer increases the efficiency of the reaction on the surface of the studied metal oxide system.*

Keywords: reaction, surface, nanoparticles, metal, oxide, carbon, tunneling, charged particles, gold, aluminum, molybdenum.

INTRODUCTION

Metal nanoparticles on oxides are used in various applications, one of which is heterogeneous catalysis [1]. This motivates extensive studies of the corresponding model catalysts on a metal/oxide substrate for a better understanding of elementary stages associated with reactions on their surface [2]. One of the key factors that activate the reactions on the surface of the applied metal particle is the amount of charge acquired by the particle due to the charge transfer between the oxide substrate and metal particle [3–5]. For example, for $Au/TiO_2(110)$, Okazaki, etc. [6] showed using DFT-calculations that for the surface enriched with titanium, the electron transfer occurs from Ti to Au. A similar situation takes place for Au applied to another oxide – MgO, for which Sanchez, *et al.*[7] showed that there is a partial electron transfer from the surface to the gold cluster, which plays a significant role in the activation of nano-sized gold clusters as catalysts of the CO oxidation reaction. Later, Goodman and his colleagues [8] also found that magnesium oxide is an effective donor of electrons for Au particles due to the charge transfer from anion vacancies (F-centers), which activates them as CO oxidation catalysts. The catalytic activation of Au particles deposited on LiF by charge transfer from anion vacancies was also recently demonstrated in [9]. The negatively charged nanoparticles of Au are believed to more actively adsorb oxygen and activate the O–O bond by charge transfer from Au [10] and also contribute to the activation of CO [11].

[1]Kabardino-Balkarian State University named after H. M. Berbekov, Nalchik, KBR, Russia, e-mail: oandi@rambler.ru; [2]North Ossetian State University named after K. L. Khetagurov, Vladikavkaz, Republic of North Ossetia – Alania, Russia, e-mail: t_magkoev@mail.ru; ketroel@gmail.com; [3]Geophysical Institute of Vladikavkaz Scientific Centre of the Russian Academy of Sciences, Vladikavkaz, Republic of North Ossetia – Alania, Russia, e-mail: vzaal@mail.ru. Translated from Izvestiya Vysshikh Uchebnykh Zavedenii, Fizika, No. 3, pp. 81–87, March, 2022. Original article submitted February 3, 2021.

In [12–16], it was found that for metal particles applied to nanostructured oxide layers grown on metal substrates, there is an additional charge-transfer channel from metal particles by means of electron tunneling through an intermediate oxide layer [12].

Given the foregoing, the purpose of this work is to study the influence of charge tunneling through the oxide film on the oxidation of carbon monoxide in the metal-oxide system. To level out foreign processes caused by the interaction of metal with an oxide and thereby masking possible tunnel effects, noble metal (Au), stable oxide (Al_2O_3), and simple well-studied reagents (CO and O_2) were selected.

EXPERIMENTAL

The studies were carried out in a modified ultrahigh vacuum system VG Escalab MII (limiting pressure of residual gases: $3 \cdot 10^{-10}$ Torr), which implemented the methods of Auger electron spectroscopy (AES) with a single-stage cylindrical analyzer with a coaxial gun, low energy electron diffraction (LEED) using four-grid electron optics, grazing incidence infrared spectroscopy (IRS), temperature-programmed desorption (TPD) using a quadrupole mass spectrometer, Anderson electron work function measurements, and atomic force microscopy (AFM). The choice of IRS is due to the fact that *p*-polarized light used in IRS provides sensitivity to vibrations of molecules located perpendicular to the plane of the adsorbent surface. This situation is realized, as a rule, for diatomic polar molecules, such as CO, which are adsorbed in vertical or inclined geometry on most metallic and nonmetallic substrates [17].

An aluminum oxide film of controlled thickness and structure was formed on the surface of a Mo(110) crystal held at an elevated temperature using the well-known procedure of reactive thermal evaporation of aluminum atoms from a Knudsen cell in an oxygen atmosphere with a partial pressure of $1 \cdot 10^{-7}$ Torr [18]. The choice of Mo(110) is due to the fact that it is a refractory metal. This makes it possible to carry out its high-temperature heat treatment, which is necessary for the formation of structurally ordered α- Al_2O_3 (1000) films. Due to the closeness of the lattice parameters of Mo(110) and α-Al_2O_3 (1000), it becomes possible to obtain epitaxial films even of very low thicknesses. The film thickness (θ) was estimated with an error of 15% by measuring the flux of aluminum atoms using a quartz resonator and by weakening the intensity of the Mo(110) MNV Auger signal (188 eV) during oxide film growth [18, 19]. The flux of deposited Al atoms was additionally controlled by changing the electron work function from the Mo(110) substrate during the growth of a submonolayer aluminum oxide film [20]. Au atoms were deposited onto an Al_2O_3 film by thermal sputtering of bulk Au (purity 99.9999%) from a Knudsen cell on substrates (300 K), followed by annealing at 500 K for 3 min to achieve an equilibrium state. The thickness of the Au coating was also determined using a quartz resonator and controlled by the weakening of the Auger signal from the substrate (O KVV, 502 eV). The surface concentration of Au atoms $1.45 \cdot 10^{15}$ cm^{-2} was taken equal to one conditional monolayer (1 MLE). High purity CO and O_2 were used in the experiments, which were vented in a controlled manner into an ultrahigh vacuum chamber (1 Langmuir (L) corresponds to 10^{-6} Torr·s). The sample holder, on which the Mo(110) crystal was mounted coaxially with a quartz resonator, allowed the sample to be cooled with liquid nitrogen to 90 K, heated to temperatures of 1000–1500 K by passing current through the sample, and heated up to 2700 K by electron bombardment.

RESULTS AND DISCUSSION

Taking into account that the probability of electron tunneling through an oxide dielectric layer depends exponentially on its thickness, measurements of the efficiency of CO oxidation on the $Au/Al_2O_3/Mo(110)$ surface were carried out at various thicknesses of aluminum oxide, namely, of 2, 4, 6, and 8 monolayers . Since the reaction on the adsorbent surface is extremely sensitive to the state of the surface, it was necessary to ensure the identity of the structural, electronic, and adsorption properties of aluminum oxide films, as well as the properties of Au/Al_2O_3 at different thicknesses of the aluminum oxide film. According to the literature data [18, 19, 21–23], an aluminum oxide film with a thickness of 2 monolayers has properties similar to those of bulk aluminum oxide. Moreover, starting from this thickness, the film acquires dielectric properties [24–26]. The LEED patterns of aluminum oxide films with thicknesses of 2, 4, 6, and 8 monolayers are almost identical and demonstrate hexagonal symmetry corresponding to α-

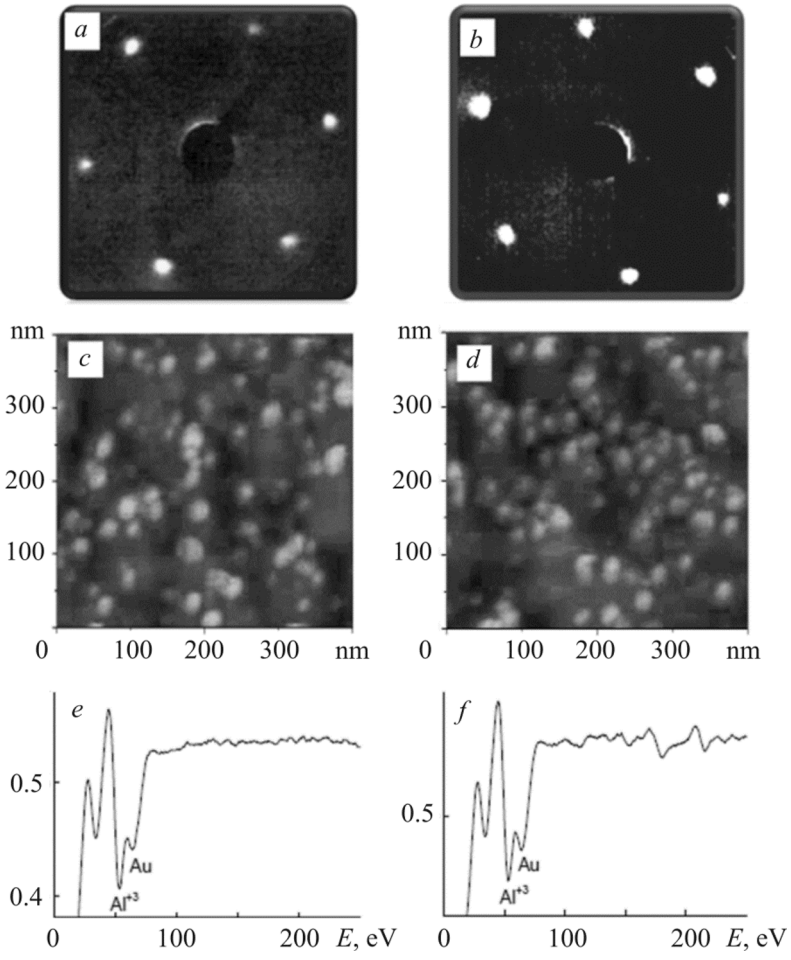

Fig. 1. LEED patterns of aluminum oxide with thicknesses of 2 (*a*) and 8 (*b*) monolayers on the Mo(110) surface. AFM images (*c*, *d*) and Auger spectra (*e, f*) of gold coating (0.7 ML) on both films.

Al_2O_3 (1000) (Fig. 1*a*, *b*), similar to that observed in [18, 19, 27]. The energy position of the Al interatomic Auger transition and its intensity with respect to the amplitude of the O KVV Auger line of oxygen are almost identical for aluminum oxide films of various thicknesses. This indicates that the stoichiometry of the oxide films is the same.

It is known [28] that the similarity of the surface state of aluminum oxide films is confirmed by studying the adsorption properties of test molecules, such as, for example, CO. The IR spectra in the range of intramolecular vibrations of CO adsorbed under a saturating coating (exposure at 200 L) on 2-, 4-, 6-, and 8-monolayer aluminum oxide films cooled to 90 K are shown in Fig. 2.

As can be seen, the spectra are similar, which indicates that the surface state of aluminum oxide films at all investigated thicknesses is almost the same. Since it is known that CO is not adsorbed on regular regions of aluminum oxide at 90 K [29], the observed IR absorption line is probably due to the fact that CO molecules are predominantly adsorbed on the oxide surface defects [30]. The same energy position of the IR absorption line, its intensity, and half-width allow us to assume that the nature of defects and their density are the same for all aluminum oxide films under study. The fairly low intensity of the IR line indicates that the density of defects is low. The most probable nature of such defects are anion vacancies, which exist to a certain extent even in case of structurally ordered predominantly stoichiometric aluminum oxide films grown by reactive deposition [31]. They stimulate the adsorption of CO molecules on the aluminum oxide surface due to the charge transfer from the negatively charged F-center of the substrate to the

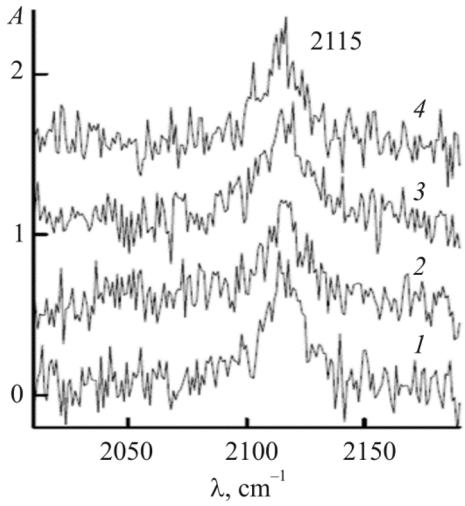

Fig. 2

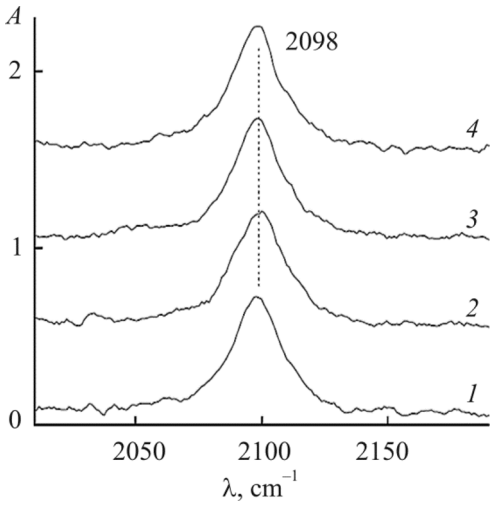

Fig. 3

Fig. 2. IR spectra of CO obtained after exposure at 200 L in CO of the surface of the 2 ML (*1*), 4 ML (*2*), 6 ML (*3*), and 8 ML (*4*) thick aluminum oxide films.

Fig. 3. IR spectra from the surface of gold clusters (0.7 ML) deposited on Al_2O_3/Mo(110) at T = 90 K after exposure in CO at 100 L. Aluminum oxide film thickness is 2 ML (*1*), 4 ML (*2*), 6 ML (*3*), and 8 ML (*4*).

antibonding 2π*-orbital of the CO molecule. This process is insignificant on regular centers of an ideal α-Al_2O_3 (1000) substrate [32].

The similarity of the morphology of the Au layers (0.7 MLE) deposited on aluminum oxide films of various thicknesses is demonstrated by AFM images (Figs. 1*c*, *d*) and confirmed by the similarity of the ratio of Auger line intensities of Au NVV and Al LVV (Figs. 1*e*, *f*) [19, 33]. According to the DFT calculations of Jennison *et al*. [34, 35], Au binds to α-Al_2O_3 (1000) by ionic bond in case of a submonolayer coating, while in case of coatings, when three-dimensional islands are formed, the polarization effect dominates in the metal–oxide bonding. A special feature of Au particles deposited on the oxide surface is that as a rule, they are neutral in regular areas of the surface [12, 36, 37].

In order to confirm whether the state of Au particles depends on the thickness of the aluminum oxide film, the adsorption of CO molecules was studied by IRS using an exposure at about 100 L. All the IR spectra recorded in this case consist of the vibrational line of CO at 2098 cm^{-1} and are almost identical to each other (Fig. 3).

The observed similarity of the IR spectra indicates the similar morphological and structural states of the Au films, regardless of the aluminum oxide film thickness. Since CO is practically not adsorbed on the regular surface of Au under the conditions used [38], the observed IR absorption line can be attributed to molecules associated with low-coordinated centers present in nanosized Au clusters, as well as to the metal/oxide interface [12, 29, 38−40]. The smaller value of the wave number of CO on Au (2098 cm^{-1}), as compared to that on the surface of aluminum oxide (2115 cm^{-1}), may be due to a higher probability of charge transfer from Au than from an oxide anion vacancy to the antibonding 2π*-orbital of the CO molecule.

The postadsorption of oxygen on the surface of the CO/Au/ Al_2O_3 system at 90 K upon exposure at 100 L leads to a violet shift of the CO absorption line by 5–6 cm^{-1} without a noticeable change in its intensity. Such insignificant change in the wave number can hardly be attributed to the displacement of the molecule to another adsorption center caused by the adsorption of oxygen. The latter would be characterized by a more significant vibrational shift [41]. Since molecular oxygen is known to dissociate on ultrasmall Au particles [3], the observed violet shift of the IR line can be explained by a decrease in the population of the antibonding 2π*-orbital of CO due to partial charge transfer to the 2*p*-level of the oxygen atom, which has a higher electron affinity [42].

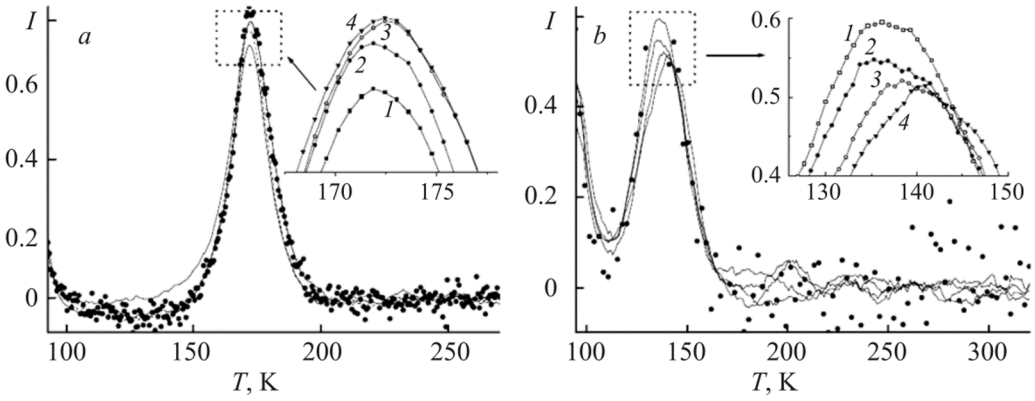

Fig. 4. TPD spectra of CO (*a*) and CO_2 (*b*) obtained by continuous exposure of the CO/Au/ Al_2O_3system in a medium with an oxygen partial pressure of 10^{-6} Torr. The inset shows the regions of TPD-peaks. Aluminum oxide film thickness is 2 ML (*1*), 4 ML (*2*), 6 ML (*3*), and 8 ML (*4*).

The observed rather low sensitivity of CO IR spectra to the O_2 post-adsorption suggests that carbon monoxide and oxygen do not compete for the adsorption site on the surface of the gold particle at 90 K. Instead, they are likely to be in neighboring adsorption sites, slightly influencing each other, which manifests itself in the observed slight violet shift of the IR absorption line. According to the calculations [43, 44], the predominant adsorption site for atomic oxygen is a cavity formed by four Au atoms, while CO binds to the atoms of the Au cluster.

A more pronounced effect, eventually leading to a molecular transformation ($CO + O_2 \rightarrow CO_2$), appears upon heating, which stimulates migration of adsorbed particles over the surface and their activation. Temperature-programmed desorption (TPD) spectra of CO and CO_2, obtained by continuous exposing the CO/Au/ Al_2O_3/Mo(110) system to oxygen (partial pressure 10^{-6} Torr), are shown in Figs. 4*a, b*. The temperature sweep rate was chosen equal to 1 K/s to ensure the equilibrium of the process, and the TPD mass spectrometer was tuned for simultaneous detection of CO (m/z = 28) and CO_2 (m/z = 44). As can be seen, along with CO desorption (Fig. 4*a*), CO_2 is also formed, although to a lesser extent (Fig. 4*b*).

A more detailed examination of the regions of the TPD-spectra maxima (the inset in Fig. 4) shows that there is a peculiarity that the intensity of the CO signal increases, and that of the CO_2 signal decreases with an increase in the oxide film thickness. This means that the efficiency of the CO oxidation is higher for a thinner alumina interlayer film. The efficiency (σ) can be qualitatively defined as the ratio of the intensities (I) of the CO_2 and CO TPD lines ($\sigma = I(CO_2)/I(CO)$). The dependence of this value on the thickness of the aluminum oxide film is shown in Fig. 5. Taking into account that the oxidation rate of CO on the surface of deposited Au clusters depends on their charge, the observed dependence can be regarded as an indication that tunneling of electrons of the Mo(110) metal substrate through the aluminum oxide film into the reaction region on the Au/Al_2O_3 increases the efficiency of CO oxidation. The reaction is realized at an excess charge, which is formed as a result of the tunneling effect from the metal substrate through the aluminum oxide layer. This agrees well with the results of the corresponding theoretical studies, which indicate that the recharge of the deposited Au cluster during the CO oxidation cycle significantly affects the energy of all redox stages in catalytic transformations [45]. In addition, according to [46], an O_2 molecule gains approximately one electron upon adsorption, and the O–O bond length, which depends on the excess charge of the molecule, increases to 1.39–1.47 Å depending on the cluster size. In addition, at the metal/oxide interface, charge redistribution occurs due to the adsorption of reagents. Theoretically, this feature is substantiated by the corresponding calculations [45], according to which, in order to implement the reaction process on the surface of metal oxide systems, an electron reservoir is required, which in the present case is the Mo(110) metal substrate, which "supplies" the charge by tunneling through Al_2O_3. This effect, however, is not dominant: as can be seen from Fig. 5, the increase in the efficiency of CO oxidation is not very significant and does not exceed 20%.

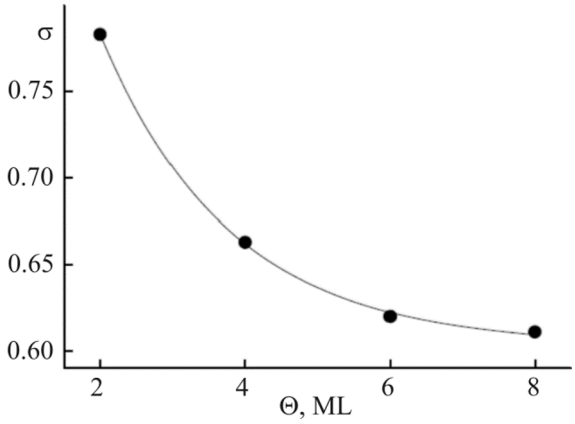

Fig. 5. Dependence of the intensity ratio of the CO_2 to CO TPD-lines on the aluminum oxide film thickness (points). An exponential approximation of the obtained dependence is shown as a continuous curve.

Taking into account the possibility of electron tunneling to Au particles through the oxide layer, it can be expected that the charge of the Au particles will manifest itself in a change of the frequency of CO IR absorption lines with a change in the oxide film thickness. The latter, however, is not true. As seen in Fig. 3, the frequency corresponding to CO is practically the same for all investigated thicknesses of the aluminum oxide film. This means that in "static" mode, tunneling can be negligible. The effect will be enhanced under reaction conditions when molecular oxidation requires intense dynamic charging/recharging of Au particles, the metal/oxide interface, and reagents.

CONCLUSIONS

The structural, morphological, and adsorption properties of Au nanoparticles on an ordered Al_2O_3 film grown on a Mo(110) substrate are similar to those for oxide films with the thicknesses of 2 to 8 monolayers. In contrast to the regular surface of bulk Au, CO is easily adsorbed on the deposited gold nanoclusters and at the metal/oxide interface at a substrate temperature of 90 K. The state of the adsorbed CO molecules rather weakly depends on the subsequent adsorption of oxygen molecules, which indicates that these molecules occupy different adsorption sites. Heating of the mixed ($CO + O_2$) layer leads to the desorption of both CO and CO_2 into the gas phase. A characteristic feature of this process is that the fraction of the desorbed CO_2 molecules relative to CO ones decreases exponentially with an increase in the thickness of the aluminum oxide film. The latter, taking into account the well-known fact that the efficiency of CO oxidation depends on the amount of excess charge acquired by the Au particle, the metal/oxide interface, and the reagents, is evidence of the fact that electron tunneling between the reaction zone and the metal substrate through the intermediate oxide layer stimulates the oxidation process of CO molecules.

The work was carried out within the framework of project No. FEFN-2021-0005 of the Ministry of Education and Science of the Russian Federation using the equipment of the Laboratory of Surface Physics and Catalysis of SOGU, as well as the project No. 19-47-02010 of the Russian Science Foundation. The authors would like to thank Professor Francisco Zaera, University of California, Riverside, for their collaboration.

REFERENCES

1. J. C. Vedrine, Metal Oxides in Heterogeneous Catalysis, Elsevier (2018).
2. S. Chen, F. Xiong, and W. Huang, Surf. Sci. Rep., **74**, 100471 (2019).
3. A. Picone, M. Riva, A. Brambilla, *et al*., Surf. Sci. Rep., **71**, 32 (2016).
4. Y. Cai and Y. P. Feng, Progr. Surf. Sci., **91**, 183 (2016).
5. K. Honkala, Surf. Sci. Rep., **69**, 366 (2014).
6. K. Okazaki, Y. Morikawa, S. Tanaka, *et al*., Phys. Rev. B, **69**, 235404 (2014).
7. A. Sanchez, S. Abbet, U. Heiz, *et al*., J. Phys. Chem. A, **103**, 9573 (1999).
8. Z. Yan, S. Chinta, A. A. Mohamed, *et al*., J. Am. Chem. Soc., **127**, 1604 (2005).
9. I. V. Tvauri, B. E. Gergieva, *et al*., Solid State Commun., **42**, 213−214 (2015).
10. G. Yoon, H. Hakkinen, and U. Landman, J. Phys. Chem. A, **107**, 4066 (2003).
11. N. Lopez, J. K. Norskov, T. V.W. Janssens, *et al*., J. Catal., **225**, 86 (2004).
12. Q. Fu and T. Wagner, Surf. Sci. Rep., **62**, 431 (2007).
13. M. Heemeier, S. Stempel, S. K. Shaikhutdinov, *et al*., Surf. Sci., **523**, 103 (2003).
14. J. Libuda, M. Frank, A. Sandell, *et al*., Surf. Sci., **384**, 106 (1997).
15. M., Baumer, J. Biener, and R. J. Madix, Surf. Sci., **432**, 189 (1999).
16. J. A. Rodriguez, M. Kuhn, and J. Hrbek, J. Phys. Chem., **100**, 18240 (1996).
17. C. J. Hirschmugl, Surf. Sci., **500**, 577 (2002).
18. D. W. Goodman, J. Vac. Sci. Technol. A, **14**, 1526 (1996).
19. M.-C. Wu and D. W. Goodman, J. Phys. Chem., **98**, 9874 (1994).
20. G. S. Grigorkina, I. V. Tvauri, *et al*., Solid State Commun., **233**, 11 (2016).
21. R. M. Jaeger, H. Kuhlenbeck, H.-J. Freund, *et al*., Surf. Sci., **259**, 235 (1991).
22. C. Becker, J. Kandler, H. Raaf, *et al*., J. Vac. Sci. Technol. A, **16**, 1000 (1998).
23. D. R. Jennison, C. Verdozzi, P. A. Schultz, and M. P. Sears, Phys. Rev. B, **59**, 15605 (1999).
24. T. T. Magkoev and G. G. Vladimirov, J. Phys.: Condens. Matter., **13**, L655 (2001).
25. T. T. Magkoev, K. Christmann, A. M.C. Moutinho, and Y. Murata, Surf. Sci., **515**, 538 (2002).
26. T. T. Magkoev, G. G. Vladimirov, D. Remar, and A. M.C. Moutinho, Solid State Commun., **122**, 341 (2002).
27. G. Frederick, G. Apai, and T. N. Rhodin, Phys. Rev. B, **44**, 1880 (1991).
28. J. L.G. Fierro and J. F.G. De La Banda, Catal. Rev., **28**, 265 (1986).
29. C. T. Campbell, Surf. Sci. Rep., **27**, 1 (1997).
30. A. Zecchina, D. Scarano, S. Bordiga, *et al.*, Catal. Today, **27**, 403 (1996).
31. G. Renaud, B. Villette, I. Vilfan, and A. Bourret, Phys. Rev. Lett., **73**, 1825 (1994).
32. M. Casarin, C. Maccato, and A. Vittadini, J. Phys. Chem. B, **106**, 795 (2002).
33. S. Ossicini, R. Memeo, and F. Ciccacci, J. Vac. Sci. Technol. A, **3**, 387 (1985).
34. A. Bogicevic and D. R. Jennison, Phys. Rev. Lett., **82**, 4050 (1999).
35. A. E. Mattsson and D. R. Jennison, Surf. Sci., **520**, L611 (2002).
36. Y. Cao, S. Hu, M. Yu, *et al*., Phys. Chem. Chem. Phys., **18**, 17660 (2016).
37. A. M. Marquez, J. Graciani, and J. F. Sanz, Theor. Chem. Acc., **126**, 265 (2010).
38. R. Meyer, C. Lemire, Sh. K. Shaikhutdinov, and H.-J. Freund, Gold Bulletin, **37**, 72 (2004).
39. R. Grisel, K. Weststrate, A. Gluhoi, and B. E. Nieuwenhuys, Gold Bulletin, **35**, 39 (2002).
40. A. Hussain, D. C. Ferre, J. Gracia, *et al*., Surf. Sci., **603**, 2734 (2009).
41. S. P. Davis, M. C. Abrams, J. W. Brauet, Fourier-Transform Spectroscopy, Academic Press, New York, London (2001).
42. G. Doyen and G. Ertl, Surf. Sci., **43**, 197 (1974).
43. A. Hussain, A. J. Muller, B. E. Nieuwenhuys, *et al*., Top Catal., **54**, 415 (2011).
44. Y.-G. Wang, Y. Yoon, V.-A. Glezakou, *et al*., J. Am. Chem. Soc., **135**, 10673 (2013).
45. M. F. Camellone, P. M. Kowalski, and D. Marx, Phys. Rev. B, **84**, 035413 (2011).
46. C. Harding, V. Habibpour, S. Kunz, *et al*., J. Am. Chem. Soc., **131**, 538 (2008).